DMD Fast Forward. Published on October 29, 2008 as doi:10.1124/dmd.108.022855
This article has not been copyedited and formatted. The final version may differ from this version.

DMD #22855

Identification and quantitation of the N-acetyl-L-cysteine S-conjugates of bendamustine and its sulfoxides in human bile after administration of bendamustine hydrochloride

Jens Teichert, Reinhard Sohr, Lothar Hennig, Frank Baumann, Konrad Schoppmeyer, Ulrich Patzak and Rainer Preiss

Institute of Clinical Pharmacology, University of Leipzig, 04107 Leipzig, Germany (J.T., F.B., R.P.); Institute of Pharmacology, Charité - University Medicine Berlin, 10117 Berlin, Germany (R.S.); Institute of Organic Chemistry, University of Leipzig, 04103 Leipzig, Germany (L.H.); Department of Internal Medicine II, University Hospital Leipzig, 04103 Leipzig, Germany (K.S.); Astellas Pharma GmbH, 81606 München, Germany (U.P.)

DMD Fast Forward. Published on October 29, 2008 as DOI: 10.1124/dmd.108.022855
This article has not been copyedited and formatted. The final version may differ from this version.

Running Title Page

Running Title: N-acetyl-L-cysteine sulfoxides of bendamustine

Corresponding author: Dr. rer. nat. Jens Teichert

Address: University of Leipzig, Faculty of Medicine

Institute of Clinical Pharmacology

Haertelstr. 16-18

04107 Leipzig

Germany

E-mail: Jens.Teichert@medizin.uni-leipzig.de

Tel.: +49-341-9724650 ; Fax: +49-341-9724659

Number of text pages: 23

Number of tables: 3

Number of figures: 6

Number of references: 22

Number of words in abstract: 250

Number of words in introduction: 640

Number of words in discussion: 1180

Nonstandard abbreviations:

amu, atomic mass unit; BM, bendamustine; COSY, Correlation Spectroscopy; HMBC, Heteronuclear Multiple Bond Coherence; HSQC, Heteronuclear Single Quantum Coherence; HPLC, High Performance Liquid Chromatography; LC-MS, Liquid Chromatography-Mass Spectrometry; LC-MS/MS, Liquid Chromatography-Tandem Mass Spectrometry; NMR, Nuclear Magnetic Resonance spectroscopy; Ala, alanine; Cys, cysteine; Glu, glutamine; Gly, glycine; Da, Dalton

DMD Fast Forward. Published on October 29, 2008 as DOI: 10.1124/dmd.108.022855
This article has not been copyedited and formatted. The final version may differ from this version.

Abstract

We recently reported the detection of mercapturic acid pathway metabolites of bendamustine, namely cysteine S-conjugates in human bile, which are supposed to subsequently undergo further metabolism. Here we describe the identification and quantitation of consecutive bendamustine metabolites occurring in human bile using authentic reference standards and the synthesis and structural confirmation of these compounds. Mass spectrometry data along with the HPLC retention data (fluorescence detection) of the synthetic reference standards were consistent with those of the metabolites found in human bile after administration of bendamustine hydrochloride to cancer patients. Analysis of the purified synthetic reference compounds showed a purity of at least 95%. Structural confirmation was achieved by 1- and 2-dimensional proton as well as carbon-13 NMR spectroscopy and mass spectrometry. A total of 16 bendamustine related compounds were detected in the bile of patients, 11 of them were recovered as conjugates. 8 conjugates have been structurally confirmed as novel mercapturic acids and sulfoxides. Biliary excretion of the sulfoxides was twice that of the mercapturate precursors. Glutathione S-conjugates of bendamustine have not been detected in bile samples indicating rapid enzymatic cleavage in humans. Both the lack of GSH conjugates and occurrence of diastereomeric sulfoxides emphasize species-related differences in the GSH conjugation of bendamustine between humans and rats. The total amount recovered in the bile as the sum of all conjugates over the period of 24 h after dosing averaged 5.2% of the administered dose. The question whether the novel metabolites contribute to urinary excretion should be target of future investigation.

DMD Fast Forward. Published on October 29, 2008 as DOI: 10.1124/dmd.108.022855
This article has not been copyedited and formatted. The final version may differ from this version.

Introduction

The anticancer agent bendamustine has been clinically used for more than 30 years in Germany as single-agent therapy or in combination with other antineoplastic drugs in a variety of dosages and regimens for the treatment of non-Hodgkin's lymphoma, chronic lymphocytic leukemia (CLL), and multiple myeloma. In March 2008, the U.S. Food and Drug Administration has approved bendamustine hydrochloride (BM HCl) for the treatment of patients with CLL. BM has a relatively mild safety profile, with myelosupression as the major dose-limiting toxicity, particularly neutropenia. The most common non-hematologic adverse events are vomiting, nausea, and pyrexia. In human ovarian and breast cancer cell lines, BM caused significantly more and more durable DNA double-strand breaks resulting in lower cross-resistance compared with other alkylators such as cyclophosphamide and melphalan (Strumberg et al., 1996). Recently, unique mechanistic features were reported for BM compared with other alkylators that involve regulation of apoptosis pathways, inhibition of specific checkpoints during mitosis and activation of base excision DNA repair (Gaul et al., 2008; Leoni et al., 2008). Although marketed in Germany for many years, reliable and valid information on the metabolism of BM have only been published in recent years. BM pharmacokinetics in humans was first published in 1985 based on data obtained after intravenous and oral administration of BM HCl in 7 tumor patients (Preiss et al., 1985). Since a main circulating metabolite had been detected in this study, metabolism via beta-oxidation analogous to that of chlorambucil was assumed for BM. About 45% of the total radioactivity administered as ^{14}C labeled BM was recovered in rat bile within 24 h indicating that biliary excretion could significantly contribute to total elimination of the drug (Bezek et al., 1991). Considerable urinary excretion of the parent compound, its hydrolysis products and the oxidized metabolite was observed in mice (Weber et al., 1991). Several fold higher concentrations were found in liver and kidney tissue of mice compared to other organs and tissues with the highest concentration in the gall bladder after intravenous administration of ^{14}C-BM (Bezek et al., 1996). Significant GSH conjugation of BM has been shown in humans as evidenced by the detection of three cysteine S-conjugates of BM in the plasma, bile, and urine of cancer patients treated with BM HCl (Teichert et al., 2005). In that study, 96% and 26% of total drug-related compounds was recovered as BM cysteine S-conjugates in the bile and urine, respectively. However, the mean

DMD Fast Forward. Published on October 29, 2008 as DOI: 10.1124/dmd.108.022855
This article has not been copyedited and formatted. The final version may differ from this version.

percentage of the BM dose recovered in urine as the sum of parent drug, its monohydroxy and dihydroxy hydrolysis product, and 5 metabolites including 3 cysteine S-conjugates within 24h was 8.3%, indicating that previous investigations may have overestimated renal excretion of the parent drug including both hydrolysis products. Since several peaks observed in the chromatograms remained unidentified in that study, consecutive metabolism of the cysteine S-conjugates followed by fecal and renal excretion was expected that warrants further examination of the metabolic pathway. More recently, considerable biliary excretion has been shown measuring excretion of radioactive labeled BM in rats (Chovan et al., 2007). The structures of 15 novel BM metabolites have been proposed by Chovan et al. based on LC-MS fragmentation spectra of bile and urine samples from rats. Oxidative phase I metabolism was shown to be mediated by CYP 1A2 as evidenced by detection of γ-hydroxy-BM and N-desmethyl-BM in human plasma, urine, and bile of cancer patients treated with BM HCl and after in vitro human liver microsomal incubations of BM HCl (Teichert et al., 2007). However**,** up to now the metabolic fate of BM in humans has not been analyzed in detail including the contribution of hepatobiliary and renal elimination to total elimination of BM. Therefore, the objective of this study was to elucidate the structure of additional metabolites formed by biotransformation of the recently described cysteine S-conjugates and to assess its contribution to total BM elimination in humans.

Materials and Methods

Materials

Reference standard 4-[5-[bis(2-chloroethyl)amino]-1-methyl-1H-benzoimidazol-2-yl]-butanoic acid hydrochloride, **1** (purity 99.0%) was a generous gift from Astellas Deutschland GmbH (Munich, Germany). Acetonitrile, water for HPLC, ammonium acetate, and acetic acid were purchased from J.T. Baker (Deventer, The Netherlands). N-acetyl-L-cysteine, L-cysteine and reduced L-glutathione were purchased from Fluka Riedel-de Haën/Sigma-Aldrich Laborchemikalien GmbH (Seelze, Germany). DMSO-d_6 was obtained from Chemotrade Chemiehandelsgesellschaft mbH (Leipzig, Germany). All other chemicals used in this study were purchased from Merck KGaA (Darmstadt, Germany). All reagents were of analytical grade and the solvents were of HPLC grade.

DMD Fast Forward. Published on October 29, 2008 as DOI: 10.1124/dmd.108.022855
This article has not been copyedited and formatted. The final version may differ from this version.

Instrumentation and Analytical Methods

Mass spectrometry

LC-MS analysis was carried out on a Finnigan (Finnigan MAT, Bremen, Germany, now Thermo Electron Corporation) SSQ-7000 single quadrupole mass spectrometer equipped with an electrospray ionization (ESI) interface coupled with a ConstaMetric 4100 MS Series pump, a SCM 1000 Vacuum Membrane Degasser, an autosampler AS 3000, and a model 3200 programmable wavelength detector (Thermo Separation Products, Riviera Beach, Florida, USA) coupled to a Digital Personal DEC 5000/25 workstation. ICL v.8.3.2 and ICIS v.8.3.0 software were used for data acquisition and data processing, respectively. HPLC separation was achieved on an Atlantis (Waters Corporation, Milford, USA) dC18 column (150 mm × 2.1 mm, 3 μm) with a gradient program at a flow rate of 0.3 mL/min as follows: time (min), %A (v/v); 0, 98; 0.2, 98; 32, 50; 34, 50; 35, 98; 60, 98. The injection volume was 20 μl and the MS was operated in the ESI positive ion mode. The auxiliary and sheath gas used was Nitrogen 4.6 (Air Liquide Deutschland GmbH, Krefeld, Germany) set to 60 and 10 psi, respectively. The turbo ion spray capillary voltage was maintained at 4.5 kV and capillary temperature was set at 220 °C. For each analyte, mass spectra were acquired using collision-induced dissociation (CID) with voltages of -10, -30, and -50 V. MS data were obtained by selected ion monitoring of the $[M+H]^+$-ion of the respective BM conjugate. Data acquisition, reduction, selected ion monitoring and peak area calculations are performed under software control by an Alpha AXP DEC 3000 Data System (Digital Equipment Corp, Maynard, MA, USA).

NMR spectroscopy

The ^1H and ^{13}C NMR spectra were recorded on a Varian Mercury plus 400 (Palo Alto, CA, USA) and a Bruker DRX-600 (Bruker BioSpin GmbH, Rheinstetten, Germany) spectrometers at 26° C using DMSO-d_6 as solvent. Residual solvent signals were used as internal chemical shift references for proton (δ_{DMSO} = 2.49 ppm) and carbon (δ_{DMSO} = 39.52 ppm) spectra. Signals were assigned by means of two-dimensional proton-proton (COSY) and proton-carbon (HMBC, edited HSQC) shift-correlation spectra.

DMD Fast Forward. Published on October 29, 2008 as DOI: 10.1124/dmd.108.022855
This article has not been copyedited and formatted. The final version may differ from this version.

Preparative HPLC

All conjugates were purified by preparative liquid chromatography using two Shimadzu LC 8 pumps (Shimadzu Corporation, Analytical Instruments Division, Kyoto, Japan) equipped either with a 250 mm x 32 mm column (I) filled with HyperPrep HS C18, 12µm, 100 A (Thermo Hypersil, Cheshire, England Hypersil, England) or a 250 mm x 30 mm column (II) packed with Vydac 218 TPB 1520 (Grace Vydac, Hesperia, CA, USA) at a flow rate of 32 mL/min. After dividing the reaction mixture in three aliquots, bulk separation of crude material was performed by injecting the aliquots onto column I. The mobile phase consisted of (A) 10 mM ammonium acetate solution and (B) acetonitrile/water 8:2 (v/v). From 0 to 20 min, a linear gradient ran from 90% A / 10% B to 20% B to remove impurities from the crude products. Main fractions were collected manually under ice cooling based on the UV signal monitored at 320 nm. Fractions from each peak, in most cases collected within 3 min periods, were concentrated under reduced pressure using a rotary vacuum evaporator. After adjusting the pH to 3.0 by adding HCl, the concentrated fractions were applied to column II in 100-200 mL aliquots for isolation of impurities. The mobile phase consisted of 10 mM HCl in water (A) and acetonitrile/10 mM HCl in water 8:2 (v/v, B). The gradient was 5-20% B in 40 min. After manual collection, purified fractions were each rotary evaporated followed by lyophilization to dryness yielding the respective BM conjugates as crystalline substances.

Analytical HPLC

Monitoring of products during chemical synthesis was performed on an HP 1090 gradient HPLC system with photo diode array (PDA) and HP 1046A fluorescence detector (Hewlett Packard, predecessor of Agilent Technologies, Palo Alto, CA, USA). A column SYNERGI 4 µ MAX-RP 80A, 250 x 2 mm equipped with a guard cartridge 4 x 2 mm (Phenomenex, Torrance, CA, USA) was used for separation. The mobile phase consisted of 0.1 mL 12M HCl in 1 L water (A) and acetonitrile/water/12M HCl 800:200:0.02 (v/v/v) (B). The gradient was 5 - 40% B in 70 min at a flow rate of 0.3 mL/min. For analysis by PDA detection, UV absorption was recorded at 233 nm. Wavelengths of the fluorescence detector were set to 328 nm (excitation) and 420 nm (emission) to monitor eluted components.

DMD Fast Forward. Published on October 29, 2008 as DOI: 10.1124/dmd.108.022855
This article has not been copyedited and formatted. The final version may differ from this version.

Quantitation of the BM metabolites in human bile was performed with an Alliance 2695 equipped with a fluorescence detector 2475 (Waters Corporation, Milford, USA) coupled to a column as above described. Solvent A was 5 mM aqueous ammonium acetate pH 3.85 adjusted with acetic acid and solvent B was 80:20 acetonitrile/solvent A (v/v). The flow rate was set to 0.25 mL/min. A 10 µl injection of each sample was injected onto column, separated and eluted using the following gradient (min, % B): 0, 2; 5, 6; 14.5, 8.5; 16, 14; 21, 18; 31, 30; 36, 31; 45, 40; 50, 45; 53, 2; 60, 2. The column temperature and the sample temperature were maintained at 30°C and 5°C, respectively. The wavelengths of the fluorescence detector were set as above described. Six-point calibration curves were fitted by weighted (1/concentration) least-squares linear regression for each conjugate in bile using the internal standard as described previously (Teichert et al., 2005).

Synthesis and Purification of Reference Compounds

The L-cysteine, N-acetyl-L-cysteine and glutathione S-conjugates were synthesized using a modified procedure similar to that previously reported (Teichert et al., 2005). Accordingly, 1.3 mmol of the thiol compound was diluted in 0.4 l of a solution containing 0.1 M sodium hydrogen carbonate and 0.2 M sodium chloride. To this solution, 0.63 mmol of the respective chloroethyl compound was added. After gentle stirring constantly at 30 °C for 22 min, the mixture was cooled to 4°C keeping in an ice bath. Alternatively, the reaction was carried out at room temperature. Completion of the reaction was assessed by monitoring offline the product formation using analytical HPLC. Then, the pH was adjusted to 5.0 by adding dropwise 2M aqueous hydrochloric acid. Product formation was monitored by analytical HPLC. Dissolved carbon dioxide gas was removed under reduced pressure before the solution was subjected to preparative HPLC as described above. For assessment of purity, the purified products were analyzed by analytical HPLC with UV detection at 233 nm after lyophilization as described in the section preparative HPLC. Furthermore, each purified product was subjected to ^{1}H, ^{13}C, $^{1}H,^{1}H$-COSY, HMQC, and HMBC NMR as well as mass spectrometric analysis.

The following compounds were synthesized in this way: **2**, **3**, and **4** by reaction of **1** with glutathione, **5**, **6**, and **7** by reaction of **1** with L-cysteine, **7** furthermore by reaction of **16** with L-cysteine, **8** by

DMD Fast Forward. Published on October 29, 2008 as DOI: 10.1124/dmd.108.022855
This article has not been copyedited and formatted. The final version may differ from this version.

reaction of **9** with L-cysteine, **9**, **10**, and **11** by reaction of **1** with N-acetyl-L-cysteine, **11** furthermore by reaction of **16** with N-acetyl-L-cysteine, and **14** by reaction of **12** with L-cysteine.

Compounds **12** and **13** were synthesized by oxidation of **9** and **11**, respectively as follows: 250 mL of 10 mM ammonium acetate solution containing 0.5 mM of the respective compound was adjusted to pH 4.8 by adding 2M HCl. To this solution, 5 mL of 30% hydrogen peroxide solution were added while stirring. The mixture was kept under stirring at room temperature and the oxidation-progress was monitored by analytical HPLC. At a maximum product yield, the reaction was stopped and the mixture was subjected to preparative HPLC and worked up in the usual way.

Compound **15** was obtained from **5** by a 2-step synthesis. The first step of the synthesis was the reaction of **5** with hydrogen peroxide as described for compounds **12** and **13**. After purification by preparative HPLC, the collected fraction containing the oxidized product was added to a solution of N-acetyl-cysteine in 0.1 M sodium hydrogen carbonate and 0.2 M sodium chloride as detailed above for compounds **2** - **11** and **14**. The final product was obtained as a crystalline solid after preparative HPLC and lyophilization as described above.

Compound **16** was obtained by hydrolysis of **1** as follows: 0.5 mol **1** hydrochloride diluted in 2 mL dimethylsulfoxide were added to a 120 mM aqueous solution of sodium hydrogen carbonate and the mixture was kept under stirring for a further 45 min at 30°C. The reaction was stopped by cooling on ice and adding 2M HCl. After the pH was adjusted to 3.0, the diluted carbon dioxide was removed under reduced pressure. Subsequent work up procedure of the reaction mixture was performed as described for the other compounds.

To prove identity of the products, minor amounts of the compounds **5**, **9**, and **12** were converted into the compounds **7**, **11**, and **13**, respectively, using the method described for synthesis of **16**.

Characterization of Reference Compounds

Purity of reference compounds was determined by HPLC, and major MS fragment ions are reported with the most abundant fragment ion produced at acid voltage of 50 V presented in bold type.

*Reference Compound **2***: 4-{5-[{2-[2-(4-amino-4-carboxy-butanoylamino)-2-(carboxymethyl-carbamoyl)-ethylsulfanyl]-ethyl}-(2-chloro-ethyl)-amino]-1-methyl-1H-benzoimidazol-2-yl}-butanoic

DMD Fast Forward. Published on October 29, 2008 as DOI: 10.1124/dmd.108.022855
This article has not been copyedited and formatted. The final version may differ from this version.

acid; Purity: 98.5% (as determined by HPLC analysis); MS: m/z $[M+H]^+$ 629.09 (calculated for $C_{26}H_{37}ClN_6O_8S$: 629.216), 500.04, 355.89, 339.88, 287.86, **176.64**.

*Reference Compound **3***: 4-{5-[bis-{2-[2-(4-amino-4-carboxy-butanoylamino)-2-(carboxymethyl-carbamoyl)-ethylsulfanyl]-ethyl}-amino]-1-methyl-1H-benzoimidazol-2-yl}-butanoic acid; Purity: 99.6%; MS: m/z $[M+H]^+$ 611.10 (calculated for $C_{26}H_{38}N_6O_9S$: 611.250), 482.09, 337.91, 287.84, **176.70**.

*Reference Compound **4***: 4-{5-[{2-[2-(4-amino-4-carboxy-butanoylamino)-2-(carboxymethyl-carbamoyl)-ethylsulfanyl]-ethyl}-(2-hydroxy-ethyl)-amino]-1-methyl-1H-benzoimidazol-2-yl}-butanoic acid; Purity: 99.5%; MS: m/z $[M+H]^+$ 900.26 (calculated for $C_{36}H_{53}N_9O_{14}S_2$: 900.323), 771.09, 642.05, 438.22, 352.23, **176.69**, 129.95.

*Reference Compound **5***: 4-{5-[[2-(2-amino-2-carboxy-ethylsulfanyl)-ethyl]-(2-chloro-ethyl)-amino]-1-methyl-1H-benzoimidazol-2-yl}-butanoic acid; Purity: 98.7%; MS: m/z $[M+H]^+$ 443.03 (calculated for $C_{19}H_{27}ClN_4O_4S$: 443.152), 295.91, 277.87, **119.86**.

*Reference Compound **6***: 4-(5-{bis-[2-(2-amino-2-carboxy-ethylsulfanyl)-ethyl]-amino}-1-methyl-1H-benzoimidazol-2-yl)-butanoic acid; Purity: 99.9%; MS: m/z $[M+H]^+$ 528.09 (calculated for $C_{22}H_{33}N_5O_6S_2$: 528.195), 380.97, 293.81, 233.84, **119.83**.

*Reference Compound **7***: 4-{5-[[2-(2-amino-2-carboxy-ethylsulfanyl)-ethyl]-(2-hydroxy-ethyl)-amino]-1-methyl-1H-benzoimidazol-2-yl}-butanoic acid; Purity: 95.1%; MS: m/z $[M+H]^+$ 425.06 (calculated for $C_{19}H_{28}N_4O_5S$: 425.186), 277.94, 259.75, **119.88**.

*Reference Compound **8***: 4-(5-{[2-(2-acetylamino-2-carboxy-ethylsulfanyl)-ethyl]-[2-(2-amino-2-carboxy-ethylsulfanyl)-ethyl]-amino}-1-methyl-1H-benzoimidazol-2-yl)-butanoic acid; Purity: 95.9%; MS: m/z $[M+H]^+$ **570.07** (calculated for $C_{24}H_{35}N_5O_7S_2$: 570.206), 422.94, 380.97, 293.98, 234.01, 161.80, 129.85, 119.86.

*Reference Compound **9***: 4-{5-[[2-(2-acetylamino-2-carboxy-ethylsulfanyl)-ethyl]-(2-chloro-ethyl)-amino]-1-methyl-1H-benzoimidazol-2-yl}-butanoic acid; Purity: 97.3%; MS: m/z $[M+H]^+$ 484.99 (calculated for $C_{21}H_{29}ClN_4O_5S$: 485.163), 356.05, 337.90, 295.91, 278.02, **161.74**, 129.87.

DMD Fast Forward. Published on October 29, 2008 as DOI: 10.1124/dmd.108.022855
This article has not been copyedited and formatted. The final version may differ from this version.

*Reference Compound **10***: 4-{5-[bis(2-(2-acetylamino-2-carboxy-ethylsulfanyl)-ethyl)-amino]-1-methyl-1H-benzoimidazol-2-yl}-butanoic acid; Purity: 99.1%; MS: m/z $[M+H]^+$ 612.14 (calculated for $C_{26}H_{37}N_5O_8S_2$: 612.216), **422.97**, 293.80, 234.12, 161.75, 129.85.

*Reference Compound **11***: 4-{5-[[2-(2-Acetylamino-2-carboxy-ethylsulfanyl)-ethyl]-(2-hydroxy-ethyl)-amino]-1-methyl-1H-benzoimidazol-2-yl}-butanoic acid; Purity: 95.4%; MS: m/z $[M+H]^+$ 467.03 (calculated for $C_{21}H_{30}N_4O_6S$: 467.196), 337.96, **277.97**, 161.77.

*Reference Compound **12***: 4-{5-[[2-(2-acetylamino-2-carboxy-ethanesulfinyl)-ethyl]-(2-chloro-ethyl)-amino]-1-methyl-1H-benzoimidazol-2-yl}- butanoic acid; Purity: 97.8%; MS: m/z $[M+H]^+$ 501.01 ($C_{21}H_{29}ClN_4O_6S$ req. 501.157), 371.92, 353.93, **321.90**, 295.99, 259.82, 245.92.

*Reference Compound **13***: 4-{5-[[2-(2-acetylamino-2-carboxy-ethanesulfinyl)-ethyl]-(2-hydroxy-ethyl)-amino]-1-methyl-1H-benzoimidazol-2-yl}-butanoic acid; Purity: 95.6%; MS: m/z $[M+H]^+$ 483.04 (calculated for $C_{21}H_{30}N_4O_7S$: 483.191), **353.96**, 335.93, 304.03, 285.87, 277.95, 245.95, 228.03.

*Reference Compound **14***: 4-(5-{[2-(2-Acetylamino-2-carboxy-ethanesulfinyl)-ethyl]-[2-(2-amino-2-carboxy-ethylsulfanyl)-ethyl]-amino}-1-methyl-1H-benzoimidazol-2-yl)-butanoic acid; Purity: 96.5%; MS: m/z $[M+H]^+$ 585.94 (calculated for $C_{24}H_{35}N_5O_8S_2$: 586.201), 456.98, 439.06, 406.94, 380.99, 352.43, **309.65**, 291.87, 259.73, 245.98, 147.85, 119.69.

*Reference Compound **15***: 4-(5-{[2-(2-Acetylamino-2-carboxy-ethylsulfanyl)-ethyl]-[2-(2-amino-2-carboxy-ethanesulfinyl)-ethyl]-amino}-1-methyl-1H-benzoimidazol-2-yl)-butanoic acid; Purity: 97.8%; MS: m/z $[M+H]^+$ 585.94 (calculated for $C_{24}H_{35}N_5O_8S_2$: 586.201), 498.79, 480.82, 449.04, 422.93, 351.93, 319.65, **309.88**, 291.74, 259.94, 246.00, 161.81, 129.75.

*Reference Compound **16***: 4-[5-(2-chloro-ethyl-2'-hydroxy-ethyl)-amino-1-methyl-1H-benzoimidazol-2-yl]-butanoic acid; no purity determined, for reaction used as crude product; MS: m/z $[M+H]^+$ 339.96 (calculated for $C_{16}H_{22}ClN_3O_3$: 340.143), 321.93, 285.96, 266.96, 245.89, 235.79, **227.89**.

*Glutathione conjugates **2**, **3**, and **4***

The typical fragmentation processes well known for glutathione conjugates were observed for the compounds **2 – 4**. Cleavage of the C-S bond was observed at either side of the sulfur atom. If the bond

DMD Fast Forward. Published on October 29, 2008 as DOI: 10.1124/dmd.108.022855
This article has not been copyedited and formatted. The final version may differ from this version.

was cleaved within the cysteine moiety, the charge resided on the BM moiety. Cleavage of the bond between the conjugation site of BM and the sulfur of cysteine occurred concomitant with the loss of the γ-glutamyl moiety (anhydroglutamic acid) with the positive charge on the peptide moiety leading to sulfenium ion formation as indicated by detection of the fragment ion at m/z 177, which was the most abundant fragment ion for the glutathione conjugates **2**, **3**, and **4**.

*Cysteine conjugates **5**, **6**, and **7***

Compounds **5 – 7** synthesized by the modified method were analyzed by LC-MS and their retention times as well as m/z were identical to those obtained by the method previously reported. Cleavage of the C-N bond was observed between the cysteine-S-ethyl residue and the tertiary nitrogen for each of the metabolites **5**, **6**, and **7**, leading to a loss of 147 Da and formation of the secondary amine fragments at m/z 296, 381, and 278, respectively. Fragment ions at m/z 278 and 260 indicate a loss of water from the secondary amine fragment of compound **5** and **7**, respectively. Occurrence of the fragment ion m/z 234 in the spectrum obtained for metabolite **6** indicates that cysteine S-bisconjugation appears to facilitate cleavage of the C-N bond. The molecular ions were the most intensive peaks for CID voltages up to 30 V. No parent molecular ion was observed for the cysteine S-conjugates increasing the CID offset to 50 V, and heterolytic fragmentation of the S-CH_2 bond between the cysteine moiety and the diethylamino group of BM with charge retained on the sulfur generating a sulfenium ($R\text{-}S^+$) ion was apparent as evidenced by the most abundant fragment ion at m/z 120. The abundance of the cysteine fragment (m/z 120) in compounds **5 – 7** was much higher than that of any of the other conjugates.

*Mercapturic acid conjugates **8**, **9**, **10**, and **11***

The mercapturic acid conjugates undergo the fragmentations discussed for the cysteine conjugates. Moreover, the occurrence of the N-acetyl-cysteine moiety was confirmed by cleavage of the S-CH_2 within the cysteine moiety leading to a neutral loss of 129 Da corresponding to acetylamino propionic acid that was found abundantly in the 50V CID spectra of all mercapturic acid conjugates. The corresponding fragment ion was observed at m/z 130. In addition, the mercapturic acids yielded the abundant fragment ion at m/z 162 assumed as N-acetyl-cysteine-sulfenium ion. The structure of the N-acetyl-dicysteine S-conjugate **8** showed a fragmentation pattern different from the monocysteine

DMD Fast Forward. Published on October 29, 2008 as DOI: 10.1124/dmd.108.022855
This article has not been copyedited and formatted. The final version may differ from this version.

conjugates of BM yielding an abundant fragment ion at m/z 423 formed by loss of the cysteine-S-ethyl group.

*Mercapturic acid sulfoxides **12**, **13**, **14**, and **15***

The fragmentation results from MS analysis were consistent with the structures assumed for the mercapturic acids oxidized at the sulfur atom of either the cysteine or the N-acetyl-cysteine moiety. Likewise all cysteine conjugates, the sulfoxides exhibited fragment ions by cleavage at either side of the sulfur. If two sulfur atoms are present in the molecule, more abundant fragment ions were observed by cleavage at the sulfoxide sides. In particular for compound **15**, parallel losses of 2-amino-propionic acid (Ala) and the N-acetyl-cysteine-S-ethyl moiety resulted in the most intensive fragment ion at m/z 310 corresponding to BM ethylsulfenic acid followed by a loss of methanesulfenic acid similarly to the fragmentation known for the monooxidized thioether bond in the cysteinyl side chain of a peptide under low energy MS conditions. In case of fission of the opposite carbon-sulfoxide bond as observed by neutral losses of cysteine sulfenic acid and the N-acetyl-cysteine-S-ethyl moiety, the resulting ethylamino radical of BM can be stabilized by aziridine formation yielding a fragment ion at m/z 260. Fragmentation pattern included further fragment ions at m/z 130 as well as 162 already described for the mercapturic acids. On the one hand, general lability of the sulfoxides was observed in low voltage CID mass spectra as indicated by significantly less abundant molecular ions compared to the spectra of the other conjugates. On the other hand, mass spectral data revealed large differences in the intensities of the molecular ions between the mono- and dicysteine sulfoxides. Least abundant molecular ions were observed for the monoacetyl-cysteine sulfoxides **12** and **13**. In Fig. 2, the mass spectra of the structurally isomeric sulfoxides **14** and **15** are presented.

The NMR signals of the BM S-conjugates were complex and partially overlapping. However, the spectra obtained from the reference compounds by two-dimensional NMR analyses do fit the anticipated structures. The NMR data for compounds **5 – 7** have been detailed in the preceding paper (Teichert et al., 2005). The chemical shifts for the other reference standards observed in the proton and carbon NMR are closely related to those for the cysteine S-conjugates **5**, **6**, and **7** and are summarized in Tables 1 and 2. Moreover, ^{1}H and ^{13}C NMR spectra of the oxidized N-acetyl-L-cysteine S-conjugates of BM showed additional signals, indicating that a mixture of diastereomers was obtained

DMD Fast Forward. Published on October 29, 2008 as DOI: 10.1124/dmd.108.022855
This article has not been copyedited and formatted. The final version may differ from this version.

by sulfur oxidation in vitro. Distinct differences and similar tendencies in the chemical shifts between the two diastereomers were observed for all sulfoxides. Thus, the chemical shifts appear as double signal sets.

γ-Hydroxy BM mercapturic acid

4-{5-[[2-(2-acetylamino-2-carboxy-ethylsulfanyl)-ethyl]-(2-chloro-ethyl)-amino]-1-methyl-1H-benzoimidazol-2-yl}-3-hydroxy-butanoic acid; MS: m/z $[M+H]^+$ 501.2 ($C_{21}H_{29}ClN_4O_6S$ req. 501.0), 483.1, 372.2, 354.1, 312.2, 294.2, 276.1, **162.1**, 130.1.

The synthesis and preparation of γ-hydroxy BM mercapturic acid was performed by reaction of N-acetyl-L-cysteine with γ-hydroxy BM (reference standard **19**) followed by preparative HPLC under the conditions as described above for the respective synthesis with BM. Due to the limited availability of reference standard **19**, the amount of γ-hydroxy BM mercapturic acid obtained by synthesis was not sufficient to perform NMR experiments. There was a significant difference of 4.4 min in the HPLC retention times between γ-hydroxy BM mercapturic acid and the structural isomeric conjugate **12**, both with molecular ions at m/z 501. Moreover, a split peak was observed in the chromatogram of γ-hydroxy BM mercapturic acid, giving the strong implication that the reaction product was a mixture of a pair of diastereomers. The second chiral center in the molecule is generated by gamma hydroxylation of the butyric acid side chain. To facilitate characterization of the metabolite structures, the chlorine isotope peaks at m/z 501.2 and m/z 503.2 containing the chlorine isotope ^{35}Cl and ^{37}Cl, respectively, were mass-analyzed by LC-MS/MS in 0.1-amu increments from 10 amu through the mass of the precursor ion. The characteristic fragment ions at m/z 162 and 130, which have also been observed after cleavage of the C-S binding at either side of the sulfur in the N-acetyl-cysteine conjugates, clearly indicate that there was no sulfoxide present in the reaction product of N-acetyl-L-cysteine with γ-hydroxy BM (**19**). This characteristic fragmentation pattern did not occur in the constitutionally isomeric sulfoxides as demonstrated by fragmentation of metabolite **12**.

Preparation of Stock Solutions and Calibration Samples

Individual stock solutions of the reference standards were prepared by dissolving adequate amounts of the conjugates in acetonitrile after structural confirmation to obtain final concentrations of about 1.0

DMD Fast Forward. Published on October 29, 2008 as DOI: 10.1124/dmd.108.022855
This article has not been copyedited and formatted. The final version may differ from this version.

mg/mL, and were stored at –20°C. Samples for calibration curves were prepared by adding standard solutions obtained by appropriate dilution of the respective stock solution with 0.01 M hydrochloric acid to 1 mL of blank bile. This yields calibration standard concentrations approximately in the range 0.1-100 µmol/mL.

Sample Preparation for Quantitative Analysis

0.05 mL of the working solution of the internal standard were added to bile samples from subjects (0.05 mL each) and diluted with 0.9 mL of 0.01 M aqueous hydrochloric acid, centrifuged at 15,000 g for 5 min. The solution was then filtered through a 0.2 µm Rotilabo® nylon supported membrane filter from Carl Roth GmbH (Karlsruhe, Germany). A 10-µL aliquot of the filtrate was injected into the HPLC system.

Subjects and Sampling Procedure

Samples were obtained from 5 subjects with cholangiocarcinoma after intravenous infusion of BM hydrochloride solution. The intravenous dose received by each patient on day 1 of the first of overall 4 cycles was 140 mg/m^2. Two temporary external nasobiliary drainages (7F, 290 cm, 8 holes; Endo-Flex, Voerde, Germany) were placed into the left and right hepatic duct, each with endoscopic retrograde cholangiography and left in place for the entire collection period. Bile was collected quantitatively before dosing and during 16 intervals up to 24 hours after starting the 30-minute infusion. 10-mL aliquots of the bile samples were stored in polypropylene tubes at -70°C until measurement. The nasobiliary drainages were removed and permanent endoscopic stenting was performed after sample collection. The Ethics Committee of the Faculty of Medicine of the University of Leipzig issued approval for this clinical trial.

Results

Characterization of BM Metabolites Observed in Human Bile

The metabolites detected in the bile are summarized in Fig. 3. The conjugates detected in the bile were designated according to their chronological order of formation followed by the hydrolysis products and phase I metabolites. A total of sixteen substances were identified in human bile, five of which were assigned as previously identified parent drug (**1**) and two hydrolysis products thereof, namely

DMD Fast Forward. Published on October 29, 2008 as DOI: 10.1124/dmd.108.022855
This article has not been copyedited and formatted. The final version may differ from this version.

monohydroxy as well as dihydroxy BM (**16**, **17**), and two oxidative metabolites (**18**, **19**). The eleven remaining metabolites were identified as cysteine S-conjugates (**5 – 7**) and their N-acetylated (mercapturic acid) as well as N-acetylated and oxidized (mercapturic acid sulfoxide) forms (**8 – 15**). Identification of the metabolites was confirmed by comparison of their retention times and molecular as well as fragment masses on HPLC with fluorescence detection and mass spectra, respectively with those of the synthesized reference substances. In addition, metabolite **12** was isolated from the bile by preparative HPLC and subsequently subjected to LC-MS analysis. Chromatogram and MS fragmentation pattern at low CID voltage of metabolite **12** isolated from human bile confirmed the results obtained by HPLC as well as LC-MS analysis of the respective synthetic reference standard indicating that this metabolite was BM mercapturic acid sulfoxide. The presence of two diastereomers for each of the sulfoxides **13** and **14** was confirmed in the bile samples by HPLC analysis showing two distinctly separated peaks. Their retention characteristics were identical to the peaks detected after chromatographic separation of the reference standards **13** and **14**, obtained by chemical synthesis. Sufficient chromatographic separation achieved for the pairs of highly polar diastereomers such as **13** and **14** diminished with increasing retention time leading to asymmetrical peak shape for the pairs of non-polar diastereomeric sulfoxides. However, the chromatographic conditions had been established to guarantee sufficient separation and quantitation of sixteen drug-related compounds from the biliary matrix.

Metabolic Profile of BM in Human Bile and Recovery of the Administered Dose

The BM metabolites **5 – 15** recovered in human bile were determined quantitatively using HPLC with fluorescence detection. Recently reported own results concerning the cysteine S-conjugates have been confirmed by measuring the highest individual maximum concentrations for the conjugates **5** and **7**, accounting for 0.35 and 0.32 mmol/L, respectively. Maximum concentrations measured for the conjugates **8**, **11**, **12**, and **13** were 5 to 10-fold lower. Representative chromatograms of bile samples collected from subjects after infusion of 140 mg/m^2 BM hydrochloride are presented in Fig. 4. Individual concentrations of BM conjugates in the bile reach a peak level approximately 60-90 min after drug administration and declined over a period of 5-6 h with exception for the sulfoxides, which

DMD Fast Forward. Published on October 29, 2008 as DOI: 10.1124/dmd.108.022855
This article has not been copyedited and formatted. The final version may differ from this version.

showed prolonged appearance. Thus, 19.5 (9.5 – 37.6) µmol was recovered in the bile as cysteine S-conjugates and 14 (9.5 – 24.9) µmol as the sum of mercapturic acids and sulfoxides. The time course for biliary excretion of the BM metabolites monitored over 24 h is shown in Fig. 5. Table 3 shows the mean amounts of BM related compounds excreted into the bile of cancer patients over the 24-h collection period after infusion of BM HCl solution. An average of 5.2% of the dose given to the subjects was cumulatively excreted into bile as conjugates over a period of 24 hours. Unchanged parent drug excreted through bile accounted for 0.03% of the administered dose in the same period. No glutathione S-conjugates of BM were detected in bile specimens collected from patients.

Discussion

Recently, we reported significant concentrations of cysteine S-conjugates in the plasma, urine, and bile of patients after administration of BM HCl (Teichert et al., 2005). Herein, the detection of consecutive metabolites of these conjugates in the bile of patients treated with BM HCl is described, which provides further evidence that GSH conjugation is a major metabolic pathway for BM in humans. We have performed structural elucidation using authentic standards previously synthesized and structurally confirmed by mass spectrometry and NMR analyses. GSH conjugation of various alkylating agents has been shown by in vitro experiments but has not been so far evidenced by in vivo identification in humans after alkylator exposure. The results of the present study are accordant with the findings of early as well as recent animal experiments in rats using radioactive labeled BM, which have shown significant biliary excretion as indicated by a recovery of 45% and 50% of the administered radioactivity in the bile and feces, respectively. (Bezek et al., 1991) (Chovan et al., 2007).

Recently, the structures of 15 novel metabolites of BM in rats have been proposed based on their mass spectral fragmentation (Chovan et al., 2007). We have detected three of these metabolites in the human bile of the patients treated with BM HCl as well and confirmed their structure as BM mercapturic acids **9**, **10** and **11**. Moreover, we have elucidated the structure of the novel mercapturic acid **8** and four sulfoxides **12 – 15** occurring in human bile, indicating CYP mediated sulfoxidation of the mercapturic acids **8**, **9** und **11**.

DMD Fast Forward. Published on October 29, 2008 as DOI: 10.1124/dmd.108.022855
This article has not been copyedited and formatted. The final version may differ from this version.

Syntheses of the novel sulfoxides by nonspecific sulfur oxidation with hydrogen peroxide yielded enantiomerically pure diastereomers due to the chiral sulfoxide derived from the enantiomerically pure (R)-sulfide **5** and the enantiomerically pure (R,R)-sulfides **9** and **11**, respectively. Occurrence of pairs of diastereomers of the conjugates **13**, **14**, and **15** in human bile was demonstrated by comparing the chromatograms of the bile samples with those of mixtures of enantiomerically pure diastereomeric sulfoxides obtained by syntheses. Chromatographic conditions used in this study were not capable of separating the diastereomers of compound **12** and therefore, no conclusion can be drawn with respect to its formation in vivo.

Furthermore, we obtained a mixture of diastereomeric γ-hydroxy-BM mercapturic acid by reaction of γ-hydroxy-BM (**19**) with N-acetyl-L-cysteine. Retention-time difference between the peaks of γ-hydroxy-BM mercapturic acid and the sulfoxide **12** was approximately the same as reported for the peaks at m/z 501 in rat urine and bile (Chovan et al., 2007). This finding indicates that these metabolites designated by Chovan et al. as oxidized mercapturic acid represent BM mercapturic acid sulfoxide **12** and γ-hydroxy-BM mercapturic acid. However, we could not detect γ-hydroxy-BM mercapturic acid in the bile samples analyzed in this study. This indicates that no significant GSH conjugation of γ-hydroxy-BM occurred in these patients.

Results obtained in this study provide evidence, on the one hand, that there are no fundamental species differences in metabolism of BM as shown by structural elucidation of several metabolites that are identical or similar to those recently proposed for rats after administration of BM HCl. Chovan and coworkers stated the mercapturic acid **10** as the major biliary metabolite in rats accounting for about 60% of total peak area. We found only minor amounts of that metabolite in human bile, while the cysteine S-conjugates, mercapturates and its sulfoxides occurred as major components. Furthermore, in apparent contradiction to the results in rats, the glutathione S-conjugates **2**, **3**, and **4** were not detectable in human bile. All together, 11 BM derived conjugates have been quantitatively determined in the human bile in this study indicating the relative importance of the GSH conjugation pathway in the metabolism of BM in humans. Four of the conjugates are novel sulfoxides. On the other hand, this result confirms the species difference between rats and humans concerning γ-GT-dependent biliary-

DMD Fast Forward. Published on October 29, 2008 as DOI: 10.1124/dmd.108.022855
This article has not been copyedited and formatted. The final version may differ from this version.

hepatic recycling. In the rat and mouse, which have relatively low levels of hepatic γ-GT, cysteine S-conjugates are preferentially formed in the intestine and kidney bearing high concentrations of γ-GT (Hinchman et al., 1991). Guinea pigs and humans can readily cleave glutathione S-conjugates due to relatively high concentrations of γ-GT in the biliary tree.

BM did not exhibit complete cross-resistance with other alkylators, for example chlorambucil and melphalan. In human ovarian and breast carcinoma cell lines, the degree of resistance to BM was lower compared with that of cyclophosphamide, melphalan, and BCNU. Moreover, BM induced more extensive and long-lasting DNA double strand breaks than other alkylators (Strumberg et al., 1996). Growth-inhibitory activities of melphalan, chlorambucil, and the phosphoramide mustard of cyclophosphamide strongly correlated with each other in a broad variety of human tumor cell lines using the National Cancer Institute in vitro antitumor screen (IVCLSP), but no significant correlation was obtained between these anticancer agents and BM (Leoni et al., 2008). Remission rates of over 55% in phase I/II studies with rather small sample sizes of 16 and 15 demonstrated good response to multi-cycle treatment with BM in patients with relapsed or refractory B-cell lymphocytic leukemia (CLL) who had been heavily pretreated with chlorambucil (Bergmann et al., 2005; Lissitchkov et al., 2006). Encouraging remission rates ranging from 73% to 83% were reported for BM after multicycle therapy in more than 100 patients with alkylator (chlorambucil, melphalan, cyclophosphamide) refractory low-grade non-Hodgkin lymphomas (Heider and Niederle, 2001; Bremer, 2002). An overall response of 77% was obtained in 76 patients with rituximab refractory predominantly stage III/IV indolent B-cell non-Hodgkin's lymphoma. Moreover, 30% of these patients had been refractory to a recent alkylator-based regimen (Friedberg et al., 2008).

The cause of these encouraging results with BM achieved in patients with alkylator-refractory lymphoid malignancies has not yet been fully explained. Besides the alkylating activity of the nitrogen mustard, possible antimetabolite activity has been discussed due to the benzimidazole heterocyclus of BM (Konstantinov et al., 2002; Schwanen et al., 2002; Leoni et al., 2008). However, this pharmacodynamic profile should be verified and further substantiated. Differences in cellular GSH-mediated detoxifying mechanism may also confer differences in therapeutic response to BM compared

with other alkylators, mainly chlorambucil and melphalan. Results from own unpublished studies with recombinant human GSTs showed that formation of monoglutathione S-BM is mediated rather by GSTA 1-1 than by GSTM 1-1, but not by GSTP 1-1. In context to this, GSH conjugation of chlorambucil is substantially mediated by GSTP 1-1 (Pandya et al., 2000; Zhang and Hanigan, 2003; Parker et al., 2008), which is the main GST-isoenzyme in lymphoid tissues (Bennaceur-Griscelli et al., 2004). Therapeutic response and resistance to therapy of BM and chlorambucil in non-Hodgkin's lymphoproliferative malignancies is currently under investigation by our group.

In conclusion, 8 novel metabolites of the GSH conjugation pathway of BM are described herein, which were structurally confirmed as mercapturates and the corresponding sulfoxides of BM. The proposed metabolic pathway of BM includes a total of 18 metabolites, inclusively the previously characterized hydrolysis products, phase I metabolites, and cysteine S-conjugates. The latter represent the major biliary metabolites of BM. Further studies should focus on renal excretion of the conjugates described herein to fully clarify their contribution to total clearance of BM in humans.

References

Bennaceur-Griscelli A, Bosq J, Koscielny S, Lefrere F, Turhan A, Brousse N, Hermine O and Ribrag V (2004) High level of glutathione-S-transferase pi expression in mantle cell lymphomas. *Clin Cancer Res* **10:**3029-3034.

Bergmann MA, Goebeler ME, Herold M, Emmerich B, Wilhelm M, Ruelfs C, Boening L and Hallek MJ (2005) Efficacy of bendamustine in patients with relapsed or refractory chronic lymphocytic leukemia: results of a phase I/II study of the German CLL Study Group. *Haematologica* **90:**1357-1364.

Bezek S, Kukan M, Scasnar V, Lukacsova M and Trnovec T (1996) Selective uptake of the anticancer drug bendamustine by liver and kidney tissues following its intravenous administration to mice. *Methods Find Exp Clin Pharmacol* **18:**117-122.

Bezek S, Scasnar V, Trnovec T and Grupe R (1991) Hepatobiliary elimination of bendamustin (Cytostasan) in rats. *Pharmazie* **46:**810-811.

Bremer K (2002) High rates of long-lasting remissions after 5-day bendamustine chemotherapy cycles in pre-treated low-grade non-Hodgkin's-lymphomas. *J Cancer Res Clin Oncol* **128:**603-609.

Chovan JP, Li F, Yu E and Ring SC (2007) Metabolic profile of [(14)C]bendamustine in rat urine and bile: preliminary structural identification of metabolites. *Drug Metab Dispos* **35:**1744-1753.

Friedberg JW, Cohen P, Chen L, Robinson KS, Forero-Torres A, La Casce AS, Fayad LE, Bessudo A, Camacho ES, Williams ME, van der Jagt RH, Oliver JW and Cheson BD (2008) Bendamustine in patients with rituximab-refractory indolent and transformed non-Hodgkin's lymphoma: results from a phase II multicenter, single-agent study. *J Clin Oncol* **26:**204-210.

Gaul L, Mandl-Weber S, Baumann P, Emmerich B and Schmidmaier R (2008) Bendamustine induces G2 cell cycle arrest and apoptosis in myeloma cells: the role of ATM-Chk2-Cdc25A and ATM-p53-p21-pathways. *J Cancer Res Clin Oncol* **134:**245-253.

Heider A and Niederle N (2001) Efficacy and toxicity of bendamustine in patients with relapsed low-grade non-Hodgkin's lymphomas. *Anticancer Drugs* **12:**725-729.

Hinchman CA, Matsumoto H, Simmons TW and Ballatori N (1991) Intrahepatic conversion of a glutathione conjugate to its mercapturic acid. Metabolism of 1-chloro-2,4-dinitrobenzene in isolated perfused rat and guinea pig livers. *J Biol Chem* **266:**22179-22185.

Konstantinov SM, Kostovski A, Topashka-Ancheva M, Genova M and Berger MR (2002) Cytotoxic efficacy of bendamustine in human leukemia and breast cancer cell lines. *J Cancer Res Clin Oncol* **128:**271-278.

Leoni LM, Bailey B, Reifert J, Bendall HH, Zeller RW, Corbeil J, Elliott G and Niemeyer CC (2008) Bendamustine (Treanda) displays a distinct pattern of cytotoxicity and unique mechanistic features compared with other alkylating agents. *Clin Cancer Res* **14:**309-317.

Lissitchkov T, Arnaudov G, Peytchev D and Merkle K (2006) Phase-I/II study to evaluate dose limiting toxicity, maximum tolerated dose, and tolerability of bendamustine HCl in pre-treated patients with B-chronic lymphocytic leukaemia (Binet stages B and C) requiring therapy. *J Cancer Res Clin Oncol* **132:**99-104.

Pandya U, Srivastava SK, Singhal SS, Pal A, Awasthi S, Zimniak P, Awasthi YC and Singh SV (2000) Activity of allelic variants of Pi class human glutathione S-transferase toward chlorambucil. *Biochem Biophys Res Commun* **278:**258-262.

Parker LJ, Ciccone S, Italiano LC, Primavera A, Oakley AJ, Morton CJ, Hancock NC, Bello ML and Parker MW (2008) The anti-cancer drug chlorambucil as a substrate for the human polymorphic enzyme glutathione transferase P1-1: kinetic properties and crystallographic characterisation of allelic variants. *J Mol Biol* **380:**131-144.

Preiss R, Sohr R, Matthias M, Brockmann B and Huller H (1985) [The pharmacokinetics of bendamustine (Cytostasane) in humans]. *Pharmazie* **40:**782-784.

Schwanen C, Hecker T, Hubinger G, Wolfle M, Rittgen W, Bergmann L and Karakas T (2002) In vitro evaluation of bendamustine induced apoptosis in B-chronic lymphocytic leukemia. *Leukemia* **16:**2096-2105.

Strumberg D, Harstrick A, Doll K, Hoffmann B and Seeber S (1996) Bendamustine hydrochloride activity against doxorubicin-resistant human breast carcinoma cell lines. *Anticancer Drugs* **7:**415-421.

Teichert J, Baumann F, Chao Q, Franklin C, Bailey B, Hennig L, Caca K, Schoppmeyer K, Patzak U and Preiss R (2007) Characterization of two phase I metabolites of bendamustine in human liver microsomes and in cancer patients treated with bendamustine hydrochloride. *Cancer Chemother Pharmacol* **59:**759-770.

Teichert J, Sohr R, Baumann F, Hennig L, Merkle K, Caca K and Preiss R (2005) Synthesis and characterization of some new phase II metabolites of the alkylator bendamustine and their identification in human bile, urine, and plasma from patients with cholangiocarcinoma. *Drug Metab Dispos* **33:**984-992.

Weber H, Amlacher R, Preiss R and Hoffmann H (1991) [Pharmacokinetics of bendamustin (Cytostasan) in B6D2F1-mice]. *Pharmazie* **46:**589-591.

Zhang L and Hanigan MH (2003) Role of cysteine S-conjugate beta-lyase in the metabolism of cisplatin. *J Pharmacol Exp Ther* **306:**988-994.

DMD Fast Forward. Published on October 29, 2008 as DOI: 10.1124/dmd.108.022855
This article has not been copyedited and formatted. The final version may differ from this version.

Legends for Figures

Fig. 1 Chemical structure of bendamustine (**1**, $C_{16}H_{21}Cl_2N_3O_2$, FW 358.27, numbering of the carbon atoms of the benzimidazole ring refers to Tables 1 and 2).

Fig. 2 ESI fragment spectra of the protonated isomers bendamustine S-cysteine-S'-mercapturic acid sulfoxide **14**, (A) and bendamustine S-cysteine-sulfoxide-S'-mercapturic acid **15**, (B).

Fig. 3 Summary of the metabolic pathway of bendamustine (BM, **1**, framed) in humans. Labeling of the metabolites detected in the bile by LC-MS refers to numbering of the reference compounds. Square brackets indicate intermediates not found in the bile. GS, glutathione-S; GSH, glutathione; GST, glutathione transferase; Cys-S, cysteine-S; γ-GT, gamma-glutamyl transferase; NAcCys-S, N-acetyl-L-cysteine-S; NAT, N-acetyl transferase.

Fig. 4 Representative chromatograms of bile collected from two patients 3-4 h after treatment with bendamustine hydrochloride.

Fig. 5 Biliary output-time (midpoint of sampling interval) data obtained for biliary excretion of bendamustine conjugates. Values are means. Error bars, depicting the standard deviation, are omitted in those three plots to improve readability and interpretation.

Fig. 6 Relative amounts of cysteine (**5**-**7**), mercapturic acid (**8**-**11**), and mercapturic acid sulfoxide (**12**-**15**) conjugates of BM excreted into bile. The parent drug, its hydrolysis products and phase I metabolites are denoted as other. Bile was collected for a total of 24 hr after administration. Values are individual.

Tables

Table 1A. Proton NMR data for the reference compounds 2-4, 8, 14, and 15.

Proton	**2**	**3**	**4**	**8**	**14**	**15**
	δ (ppm)	**δ (ppm)**	**δ (ppm)**	**δ (ppm)**	**δ (ppm)**	**δ (ppm)**
NH_2	8.55 (2H, d [br])	8.52 (2H, d [br])	[2]	6.65 (2H, s [br])	[2]	[2]
CH_2NH	8.50 (1H, t)	8.48 (1H, t)	8.51 (1H, t)	-	-	-
CHN*H*	8.39 (1H, d)	8.35 (1H, d)	8.38 (1H, d)	8.35 (1H, d)	8.55/8.56 (1H, d)	8.28/8.27 (1H, d)
H-4	7.71 (1H, d)	7.80 (1H, d)	7.44 (1H, d)	7.68 (1H, d)	7.60 (1H, d)	7.46 (1H, d)
H-3	7.08 (1H, dd)	7.29 (1H, dd [br])	6.86 (1H, dd)	7.06 (1H, dd)	7.03 (1H, dd)	6.93 (1H, dd)
H-1	6.89 (1H, d)	7.21 (1H, d [br])	6.83 (1H, d)	6.85 (1H, d)	6.94 (1H, d)	6.95 (1H, d)
C*H*NH	4.50 (1H, m)	4.45 (2H, m)	4.49 (1H, m)	4.39 (1H, m)	4.59/4.49 (1H, [1])	4.40/4.38 (1H, [1])
CH_2CHNH_2	3.90 (1H, [1])	3.87 (2H, [1])	3.71 (1H, [1])	4.15 (1H, [1])	4.01 (1H, t)	3.91/3.90 (1H, [1])
NCH_3	3.89 (3H, s)	3.90 (3H, s)	3.76 (3H, s)	3.87 (3H, s)	3.82 (3H, s)	3.74 (3H, s)
$SOCH_2CH_2$	-	-	-	-	3.78 (2H, [1])	3.74 (2H, [1])
$NHCH_2COOH$	3.76 (2H, d)	3.73 (4H, d)	3.73 (2H, [1])	-	-	-
CH_2Cl	3.74 (2H, t)	-	-	-	-	-
CH_2CH_2Cl	3.74 (2H, t)	-	-	-	-	-

GS or cys SCH_2CH_2	3.61 (2H, t)	3.65 (4H, t)	3.51 (2H, t)	3.65 (2H, t)	3.57 (2H, [1])	-
N-acetyl-cys SCH_2CH_2	-	-	-	3.59 (2H, t)	-	3.52 (2H, [1])
CH_2OH	-	-	3.54 (2H, t)	-	-	-
CH_2CH_2OH	-	-	3.42 (2H, t)	-	-	-
$SOCH_2CH_2$	-	-	-	-	3.16/2.96 (2H, [1])	3.23/3.02 (2H, [1])
het-CH_2	3.15 (2H, t)	3.17 (2H, t)	2.99 (2H, t)	3.14 (2H, t)	3.04 (2H, t)	2.94 (2H, t)
CH_2CHNH	-	-	-	2.97/2.80 (2H, [1])	3.31/3.00; 3.15 (2H, [1])	2.94/2.78 (2H, [1])
CH_2CHNH_2	2.96/2.70 (2H, [1])	2.94/2.68 (4H, [1])	2.99/2.70 (2H, [1])	3.15 (2H, [1])	3.12 (2H, [1])	3.27/3.22 (2H, [1])
GS or cys SCH_2CH_2	2.72 (2H, t)	2.68 (4H, t)	2.73 (2H, t)	2.78 (2H, [1])	2.78 (2H, [1])	-
N-acetyl-cys SCH_2CH_2	-	-	-	2.72 (2H, [1])	-	2.70 (2H, t)
CH_2CH_2CONH	2.46/2.33 (2H, [1])	2.44/2.31 (4H, [1])	2.40/2.36 (2H, [1])	-	-	-
CH_2CH_2COOH	2.40 (2H, t)	2.40 (2H, t)	2.37 (2H, t)	2.39 (2H, t)	2.38 (2H, t)	2.36 (2H, t)
CH_2CH_2CONH	2.08/2.04 (2H, [1])	2.06/2.02 (4H, [1])	2.05/1.98 (2H, [1])	-	-	-
CH_2CH_2COOH	2.01 (2H, m)	2.01 (2H, m)	1.98 (2H, m)	2.00 (2H, m)	1.98 (2H, m)	1.96 (2H, m)
CH_3CO	-	-	-	1.85 (3H, s)	1.81/1.84 (3H, s)	1.84 (3H, s)

Table 1B. Proton NMR data for the reference compounds 9-13.

Proton	**9**	**10**	**11**	**12**	**13**
	δ (ppm)	**δ (ppm)**	**δ (ppm)**	**δ (ppm)**	**δ (ppm)**
CHN*H*	8.32 (1H, d)	8.32 (2H, d)	8.32 (1H, d)	8.53/8.50 (1H, d)	8.54/8.52 (1H, d)
H-4	7.68 (1H, d)	7.67 (1H, d)	7.65 (1H, 1)	7.13/7.12 (1H, [1])	7.69/7.68 (1H, d)
H-3	7.06 (1H, dd)	7.03 (1H, dd)	7.04 (1H, dd)	7.73/7.72 (1H, [1])	7.10 (1H, m)
H-1	6.84 (1H, d)	6.81 (1H, d)	6.83 (1H, d)	6.96/6.95 (1H, [1])	6.94 (1H, [1])
C*H*NH	4.39 (1H, m)	4.39 (2H, m)	4.39 (1H, m)	4.59/4.48 (1H, [1])	4.59/4.47 (1H, [1])
NC*H*$_3$	3.88 (3H, s)	3.87 (3H, s)	3.87 (3H, s)	3.89 (3H, s)	3.88 (3H, s)
SOCH$_2$C*H*$_2$	-	-	-	3.85 (2H, [1])	3.82 (2H, [1])
C*H*$_2$Cl	3.76 (2H, [1])	-	-	3.77 (2H, [1])	-
C*H*$_2$CH$_2$Cl	3.76 (2H, [1])	-	-	3.77 (2H, [1])	-
N-acetyl-cys SCH$_2$C*H*$_2$	3.62 (2H, [1])	3.58 (4H, t)	3.57 (2H, [1])	-	-
C*H*$_2$OH	-	-	3.55 (2H, [1])	-	3.57 (2H, [1])
C*H*$_2$CH$_2$OH	-	-	3.48 (2H, [1])	-	3.50 (2H, [1])
SOC*H*$_2$CH$_2$	-	-	-	3.13/3.02; 2.87 (2H, [1])	3.15/3.01; 2.98 (2H, [1])
het-C*H*$_2$	3.14 (2H, t)	3.13 (2H, t)	3.12 (2H, t)	3.14 (2H, t)	3.11 (2H, t)

C*H*$_2$CHNH	2.97/2.79 (2H, [1])	2.96/2.80 (4H, [1])	2.96/2.79 (2H, [1])	3.30/3.02; 3.12 (2H, [1])	3.30/3.02; 3.11 (2H, [1])
N-acetyl-cys SC*H*$_2$CH$_2$	2.72 (2H, [1])	2.71 (4H, t)	2.71 (2H, t)	-	-
CH$_2$C*H*$_2$COOH	2.40 (2H, t)	2.40 (2H, t)	2.39 (2H, t)	2.39 (2H, t)	2.39 (2H, t)
C*H*$_2$CH$_2$COOH	2.00 (2H, m)	1.99 (2H, m)	1.99 (2H, m)	1.99 (2H, m)	1.99 (2H, m)
C*H*$_3$CO	1.85 (3H, s)	1.84 (6H, s)	1.85 (3H, s)	1.83/1.81 (3H, s)	1.83/1.81 (3H, s)

(400 MHz, 600 MHz, DMSO-d$_6$, ^{1}H, H,H-COSY); splitting patterns denotation as s, singlet; d, dublet; dd, double dublet; t, triplet; m, multiplet, [br], broad; chemical shifts in ppm; [1] not assigned either due to broadening or signal overlapping; [2], not observed (H-D exchange).

Table 2. Carbon NMR data for the reference compounds 2-4 and 8-15.

Carbon	**2**	**3**	**4**	**8**	**9**	**10**	**11**	**12**	**13**	**14**	**15**
	δ (ppm)	**δ (ppm)**	**δ (ppm)**	**δ (ppm)**	**δ (ppm)**	**δ (ppm)**	**δ (ppm)**	**δ (ppm)**	**δ (ppm)**	**δ (ppm)**	**δ (ppm)**
CH_2CH_2*C*OOH	173.79	173.96	173.99	173.75	173.74	173.76	173.76	173.74	173.75	173.89	174.10
CH*C*ONH	171.23	170.76*	170.69	-	-	-	-	-	-	-	-
NHCH*C*OOH	-	-	-	172.09	-	-	-	-	-	172.03/171.67	172.28/172.25
CH*C*OOH	170.97*	171.08	171.07*	-	172.11	172.12	172.12	171.78/171.60	172.01/171.62	-	-
$NHCH_2$*C*OOH	170.73*	170.81*	171.00*	-	-	-	-	-	-	-	-
CH_2*C*ONH	170.66	171.43	171.51	-	-	-	-	-	-	-	-
CH_3*C*O	-	-	-	169.61	169.51	169.57	169.57	169.73/169.33	169.77/169.38	169.79/169.42	169.59/169.57
NH_2CH*C*OOH	-	-	-	169.50	-	-	-	-	-	169.66/169.62	168.85/168.82
C-6	151.68	152.69	152.77	151.49	151.57	151.48	151.29	151.77	151.48	152.30	153.28
C-2	145.74	143.50br	145.09	145.73	145.86	145.79	146.42	145.87/145.83	146.50/146.46	145.22/145.31	144.38/144.28
C-7	131.66	131.48	138.04	131.69	131.65	131.71	131.73	131.57	131.60	134.52	138.24
C-5	124.69	126.68br	126.33	124.47	124.48	124.41	124.14	124.78	124.39	125.79	127.40
C-4	113.58	114.04	111.35	113.48	113.47	113.46	113.25	113.47	113.25	112.63	111.54
C-3	112.56	114.83br	110.66	112.46	112.29	112.34	112.20	112.74	112.64	112.45	111.90

C-1	94.72	98.04[br]	97.72	94.48	94.35	94.34	93.96	95.04	94.57	97.03	99.89
CH_2OH	-	-	58.33	-	-	-	58.05	-	57.93	-	-
CH_2CH_2OH	-	-	53.42	-	-	-	53.38	-	53.39/53.36	-	-
SO*C*H_2CHNH	-	-	-	-	-	-	-	53.15/52.85	53.22/52.87	53.24/52.89	51.66/51.44
CH_2CH_2Cl	52.49	-	-	-	52.37	-	-	52.40/52.36	-	-	-
*C*HNH	52.46	52.48	52.57	-	52.29	52.32	52.31	-	-	-	-
NH*C*HCOOH	-	-	-	52.33	-	-	-	-	-	47.36/47.03	52.39
*C*HNH_2	51.64	51.78	51.35	52.14	-	-	-	47.24/46.94	47.29	52.41	49.47/48.67
N-acetyl-cys SCH_2*C*H_2	-	-	-	51.00*	51.03	51.06	51.45	-	-	-	51.80
GS or cys SCH_2*C*H_2	51.18	52.57	51.66	50.92*	-	-	-	-	-	51.10	-
SO*C*H_2CH_2	-	-	-	-	-	-	-	48.76/48.66	48.91/48.68	49.25/48.96	49.96/49.27
SOCH_2*C*H_2	-	-	-	-	-	-	-	44.23/44.11	44.65/44.58	44.34/44.26	44.57
CH_2Cl	41.21	-	-	-	41.18	-	-	41.11	-	-	-
NH*C*H_2	40.87	40.99	40.88	-	-	-	-	-	-	-	-
S*C*H_2CHNH	33.89	33.99	34.08	33.12	33.10	33.14	33.11	-	-	-	32.87
CH_2*C*H_2COOH	32.68	32.80	32.82	32.62	32.58	32.60	32.51	32.58	32.62	32.73	33.21
S*C*H_2CHNH_2	-	-	-	31.53	-	-	-	-	-	31.74	-

N*C*H$_3$	31.11	31.38	30.07	31.03	31.00	31.00	30.97	31.02	31.00	-	30.13
CH$_2$*C*H$_2$CO	30.90	30.98	31.36	-	-	-	-	-	-	-	-
GS or cys S*C*H$_2$CH$_2$	28.27	27.90	28.70	28.88	-	-	-	-	-	28.76	-
N-acetyl-cys S*C*H$_2$CH$_2$	-	-	-	28.58	28.52	28.62	28.34	-	-	-	28.82
*C*H$_2$CH$_2$CO	26.18	26.24	26.61	-	-	-	-	-	-	-	-
het-CH$_2$	24.12	24.34	24.89	24.07	24.05	24.08	24.06	24.06	24.05	24.49	25.05
*C*H$_3$CO	-	-	-	22.45	22.42	22.44	22.44	22.42/22.39	22.44/22.39	22.45/22.41	22.45
*C*H$_2$CH$_2$COOH	21.69	21.76	22.07	21.62	21.57	21.44	21.61	21.59	21.63	21.79	22.01

(100 MHz, DMSO-d$_6$, APT, HMSC, HMBC); [br] broad, [*] could not be assigned unambiguously

Table 3. Total amounts of the compounds excreted into bile during 24 hr after intravenous administration of 140 mg/m^2 BM hydrochloride in 5 cancer patients. Values are means ± SD (standard deviation).

Compound	**1**	**5**	**6**	**7**	**8**	**9**	**10**	**11**	**12**	**13**	**14**	**15**	**16**	**17**	**18**	**19**
Amount (μmol)	0.19	9.28	1.50	8.68	1.04	0.95	0.12	2.38	2.34	5.88	1.20	0.11	0.28	0.33	0.23	0.12
SD	0.06	4.93	1.00	6.32	0.39	0.41	0.15	1.64	1.25	3.47	0.57	0.11	0.11	0.25	0.14	0.09

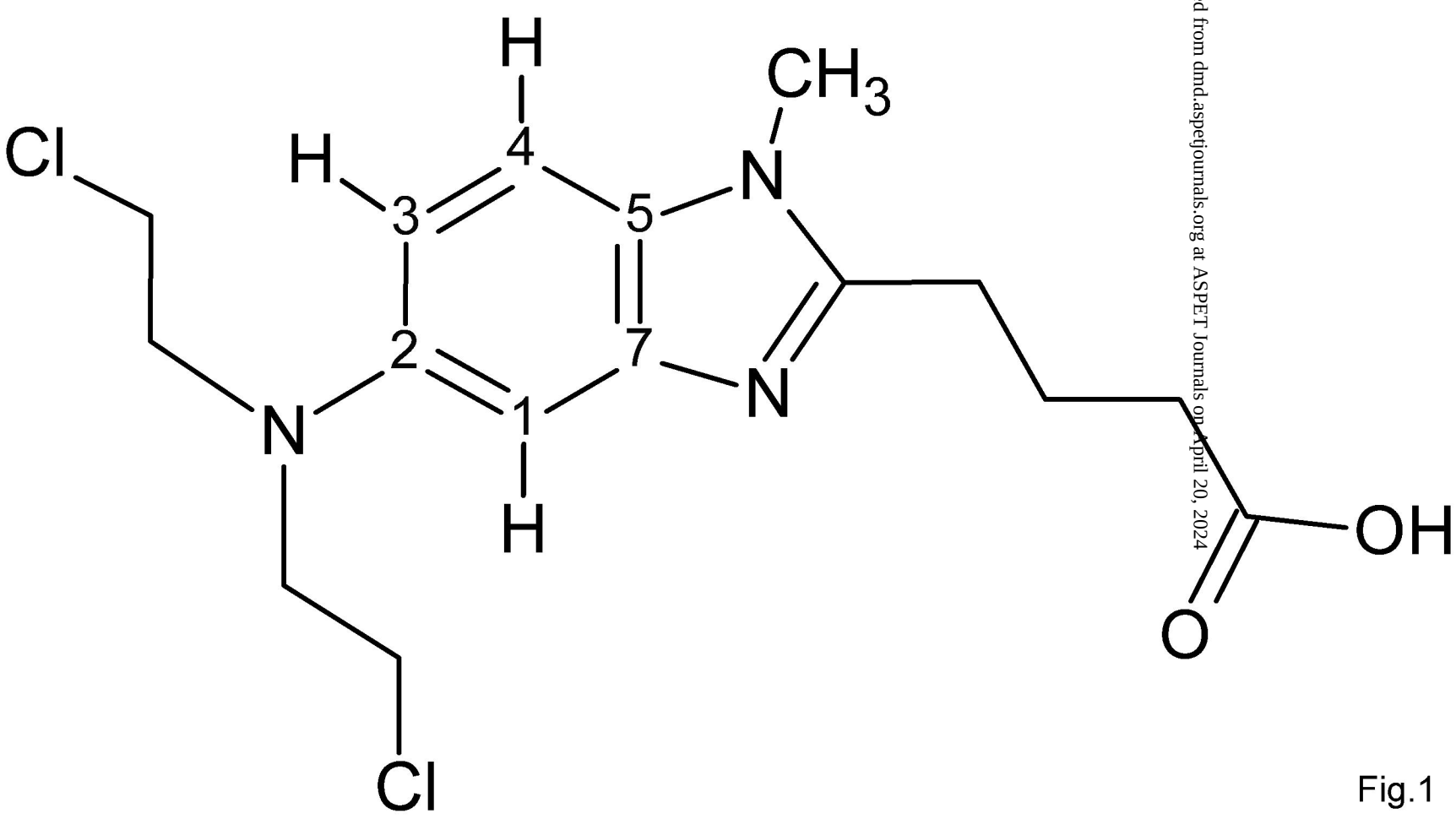

Fig.1

DMD Fast Forward. Published on October 29, 2008 as DOI: 10.1124/dmd.108.022855
This article has not been copyedited and formatted. The final version may differ from this version.

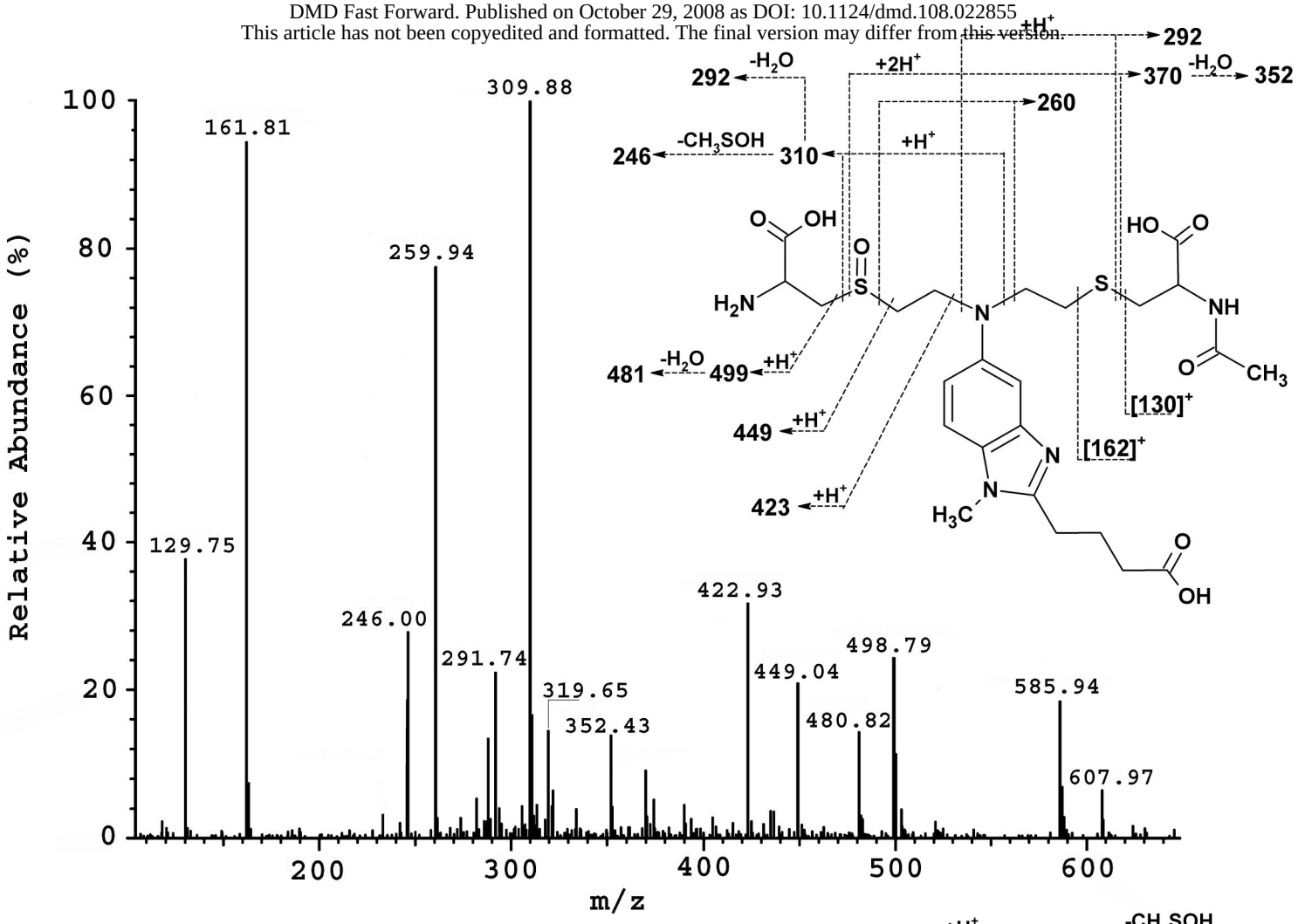

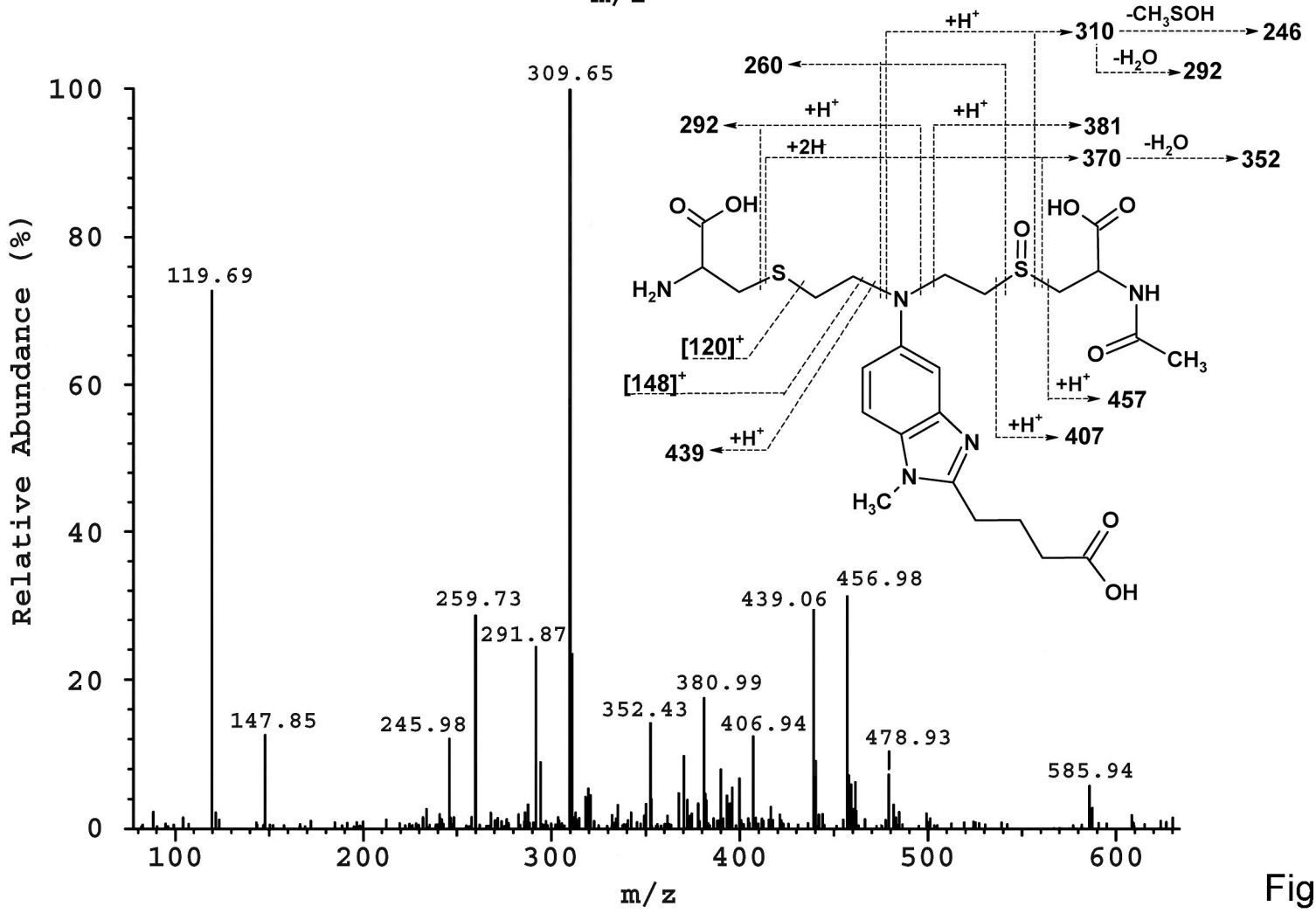

Fig.2

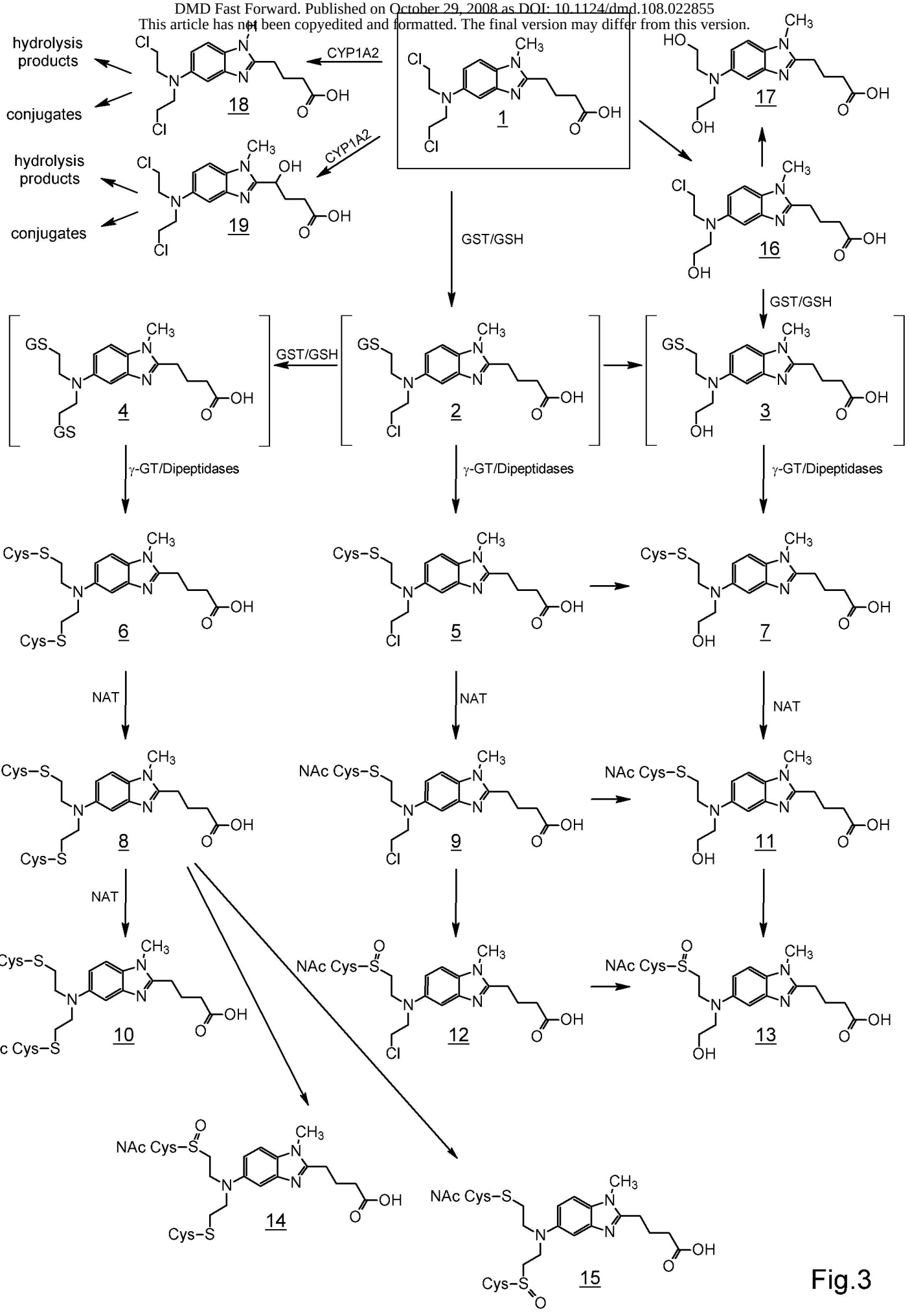

Fig.3

DMD Fast Forward. Published on October 29, 2008 as DOI: 10.1124/dmd.108.022855
This article has not been copyedited and formatted. The final version may differ from this version.

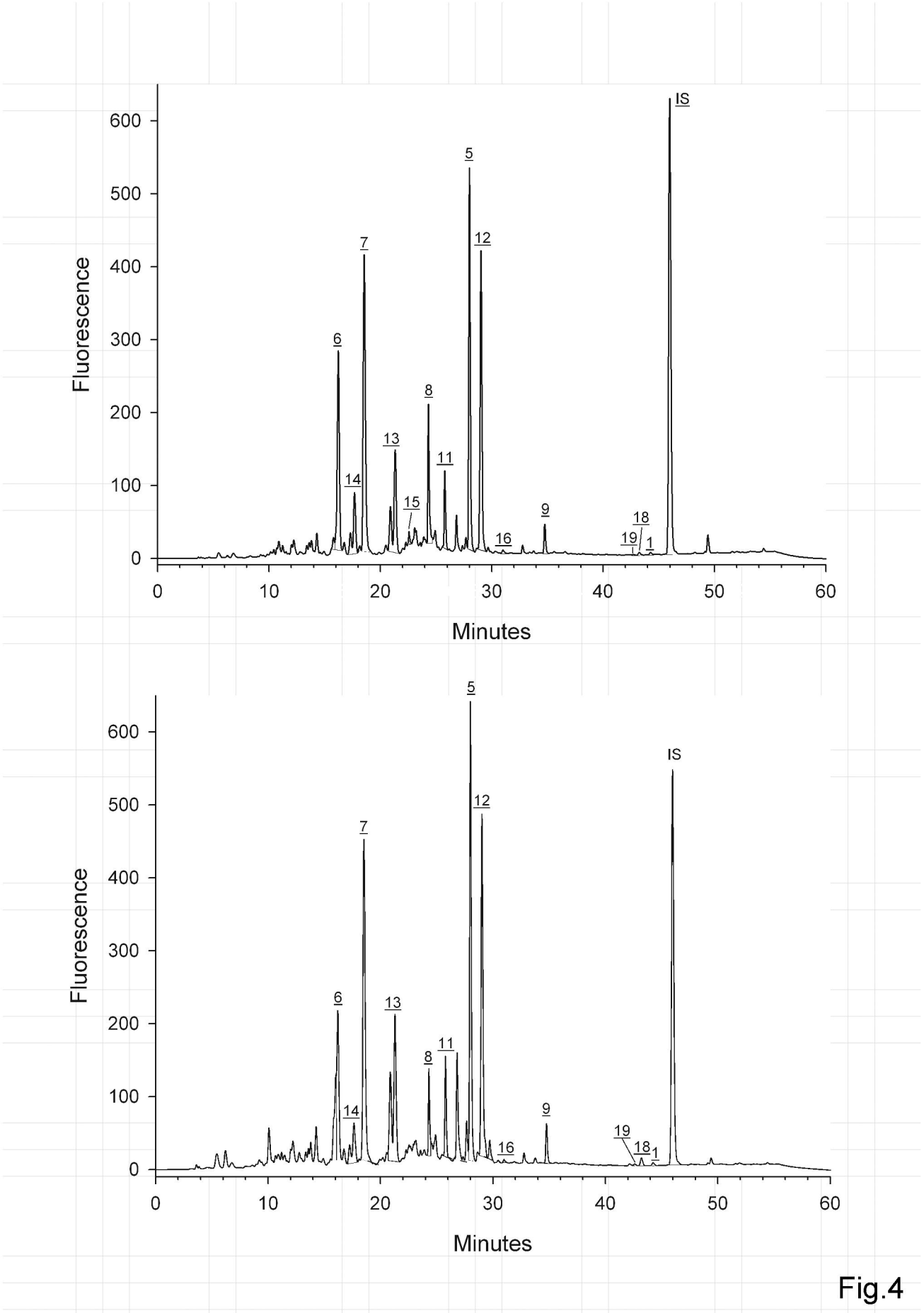

Fig.4

DMD Fast Forward. Published on October 29, 2008 as DOI: 10.1124/dmd.108.022855
This article has not been copyedited and formatted. The final version may differ from this version.

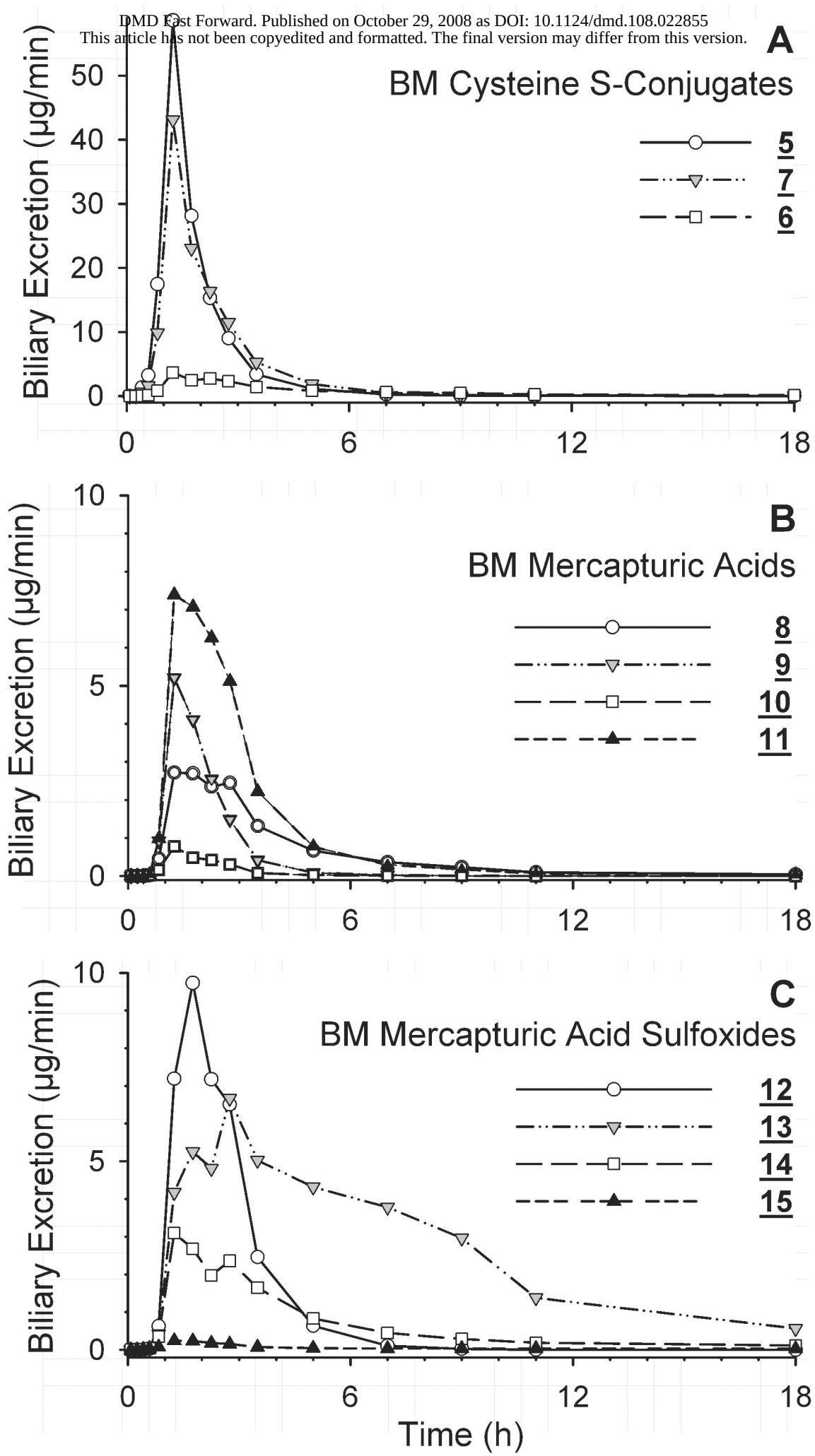

Fig.5

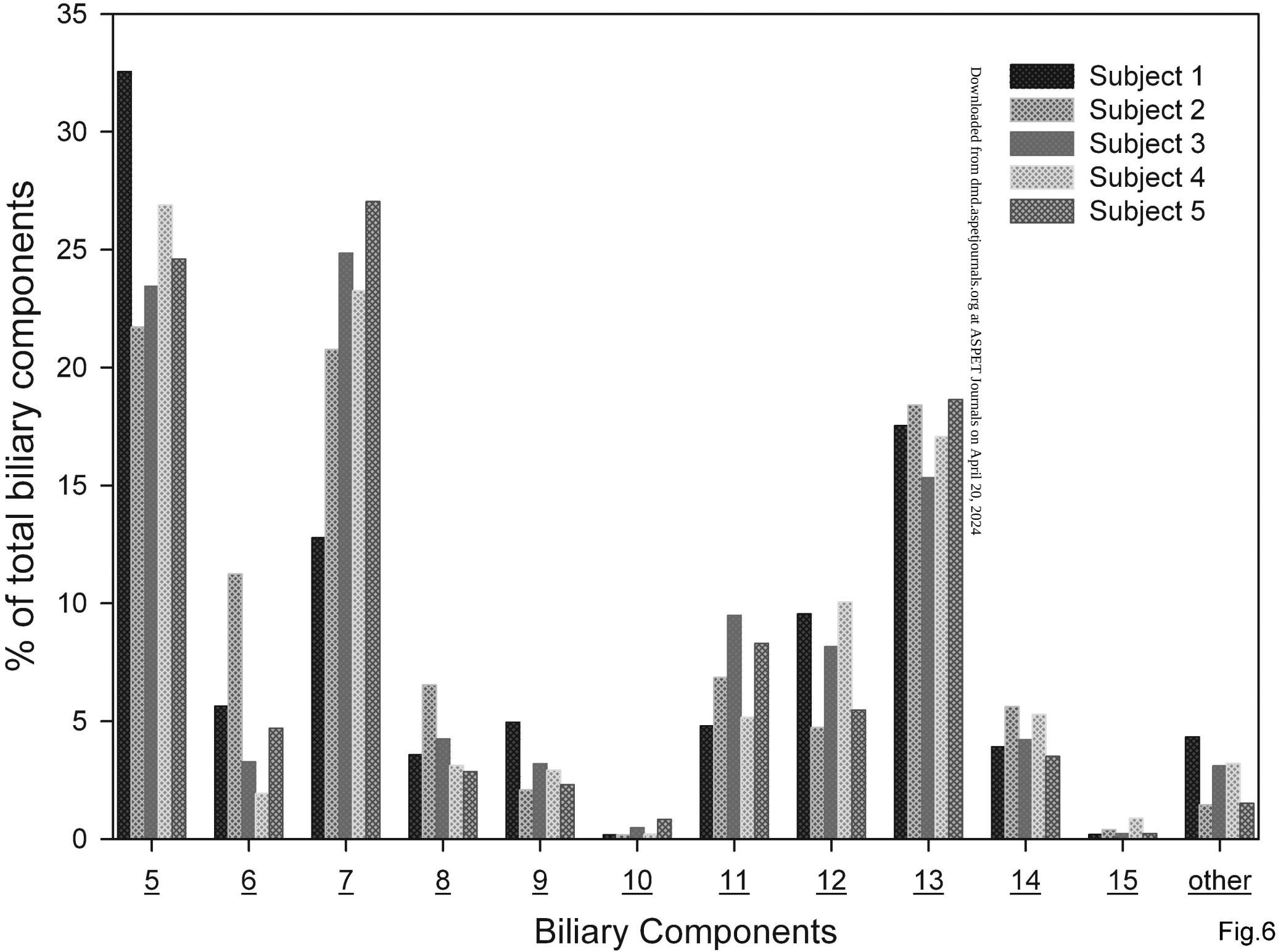

Fig.6